Fast-Flame to Detonation Transition in a Round Tube

Maddy Moran and Gaby Ciccarelli
Queen's University
Kingston, Ontario, Canada

1 Introduction

The distance required for flame acceleration and deflagration-to-detonation transition (DDT) in a channel is proportional to the channel transverse dimension. For prototypic scales this requires a channel of substantial length. To reduce the so-called DDT run-up distance, a fast-flame can be generated from the interaction of a detonation wave with a perforated plate. Chao et al. [1] performed a study in 300-mm square and 150-mm round channels and demonstrated that immediately after the perforated plate the shock-flame complex propagated at a velocity equal to one-half the CJ detonation velocity, i.e., $\frac{1}{2}V_{CJ}$. They proposed that during this initial phase, the propagation was independent of the channel geometry (round or square) and scale of the turbulence which is governed by the perforated plate hole diameter. Saif et al. [2] showed that the combustion wave after the perforated plate is a CJ deflagration. Chao et al. [1] proposed that DDT was independent of the channel geometry when the hole size was small compared to the channel width, e.g. for larger holes of 25 mm wall-effects played a role in DDT. In this geometry, DDT phenomenon has been studied using schlieren photography in rectangular narrow channels [2, 3]. These "2D experiments" suppress 3D effects leading to DDT. Monnier et. al [4] studied detonation initiation in a tube, both round and square, downstream of a single-orifice plate, where the hole was round or square. They found that detonation initiation occurred due to shock collisions at the channel axis in the round tube and in the corners of the square cross-section tube, highlighting the role of channel geometry in the initiation process. Recently, Moran and Ciccarelli [5] demonstrated using stereo-visualization and soot foils in a 76 mm square channel with a perforated plate with 6.4 mm holes that DDT occurred primarily at the channel walls. In most cases, DDT occurred in the corners where transverse shock wave focusing, and 3D boundary layer effects are important. A similar finding was made in a study performed in a smaller 25 mm square channel [6].

To mitigate the effects of the channel corners, experiments in this study were conducted in a round tube with the same perforated plate characteristics as in [5]. Stereo-visualization was once again used to precisely determine the location of DDT. The objective of the study is to compare the DDT results obtained in round and square cross-section channels of identical transverse dimensions. This approach allows for the isolation of corner effects and aims to determine whether DDT occurs at or away from the tube wall [7], a key factor in deducing the DDT mechanism.

2 Experimental set-up

Correspondence to: gaby.ciccarelli@queensu.ca

The test channel consisted of three round tube sections, all with an ID of 7.62 cm (see Fig. 1). The first section was 151 cm long and the first 138 cm of the section was filled with eighteen 50% blockage ratio orifice plates to generate a detonation wave. The remainder of this section and the following 61 cm long section were empty such that the detonation wave can stabilize. A 77.4 % blockage ratio perforated plate consisting of thirty-two 6.4 mm holes arranged in a grid pattern (see Fig. 1) was located at the beginning of the final 122 cm long tube section. The DDT phenomena was observed in this final section free of obstructions. The perforated plate was designed such that the hole spacing and layout, and number of holes closely resembled that of the square channel experiment.

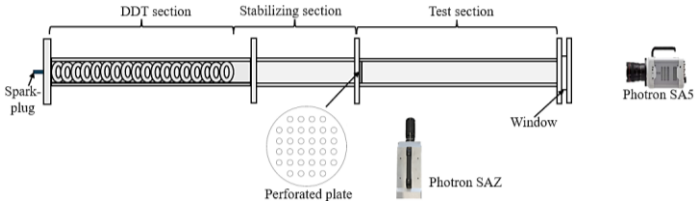

Figure 1: Experimental configuration.

Fuel-oxygen mixtures were prepared by method of partial pressure and mixed for 30 minutes. A spark-plug, and in some cases a glow-plug, were used for ignition at the closed-end. Simultaneous high-speed direct photography from a side- and end-view was captured with Photron SAZ and SA5 cameras, respectively. A Shimadzu HPV-X2 was used in a limited number of tests. The luminescence produced by the reaction zone allowed for the evolution of the flame to be investigated from a side-view and the DDT location with respect to the cross-section of the tube was investigated from the end-view photography. This set-up allowed for the precise location of the DDT event to be determined. Soot foils that wrapped the circumference of the tube were used to obtain a record of the cell structure evolution. For some tests, a soot foil was wrapped around one-half the circumference of the tube on the opposite side of the side-view camera permitting the tracking of the combustion front via the incandescence of the fine soot particles lifted by the passage of the lead shock wave and heated by the combustion products. A 430 nm ± 10 nm narrowband filter (corresponding to CH emissions) was used for end-view and side-view soot foil tests to reduce the amount of light entering the camera lens. Tests where primarily performed with stoichiometric propane-oxygen. Limited tests with propane-oxygen and hydrogen-oxygen with 40% argon-dilution were also performed.

3 Results and Discussion

3.1. Detonation Initiation Modes

3.1.1. Shock dynamics downstream from the perforated plate

The perforated plate in this study was designed to closely match that used in [5]. As seen in Fig. 1, the holes along the periphery are arranged such that four sets of two holes are closer to the channel wall than the remaining periphery holes. Extensive tests with end-view photography revealed that the hole orientation of the perforated plate influenced the shock dynamics downstream from the perforated plate. The shocks emanating from each hole interact with each other. For very reactive conditions, such a collision can result in “prompt” detonation initiation [5], these are not the focus of this study. Wall-reflection occurs first for the shocks from the four sets of holes producing an ‘X’ pattern shock structure 9 cm downstream from the perforated plate, see Fig. 2b image 2. Shocks are visible due to light generated by the high temperature shock-compressed product gas. The ‘X’ intersects with the tube wall at the same cross-sectional location as the four sets of holes in question. The shocks subsequently converge at roughly the centerline of the tube resulting in detonation initiation, similar to that observed for a single orifice hole [4]; if not, initiation often occurred from subsequent shock reflection at the tube wall. To investigate the effect of the hole configuration on detonation initiation, a limited number of tests were performed with a perforated plate with the same size and number of holes but a radially symmetric hole

pattern. Although the shock collisions after the perforated plate differed, the near-symmetric shock implosion at the center of the tube and subsequent reflection at the wall was universal.

3.1.2. Wall Detonation Initiation

Figure 2 shows select frames captured simultaneously from a side- and end-view for a $C_3H_8+5O_2$ test at an initial pressure of 5.5 kPa. The turbulent flame structure is seen in image 1 side-view (Fig. 2a), and the bright 'X' shock pattern discussed in *3.1.1.* is observed in the corresponding end-view image. In end-view image 2 (Fig. 2b), shock focusing at the tube center generates a high temperature (and pressure) region, but no detonation forms. Rather, a detonation is initiated between images 2 and 3 due to shock reflection at the channel wall. The local detonation front is clearly seen in both end- and side-view image 3. The end-view image shows that initiation occurred at roughly the 9 o'clock tube wall position. The size of the detonation bubble from the end-view is the same as that observed at centerline in the side-view. The DDT run-up distance was measured to be 15.2 cm downstream from the perforated plate. Image 4 end-view shows the detonation propagating azimuthally along the channel wall in the clockwise and counterclockwise directions. Further, the detonation also propagates radially across the tube indicating that the flame is decoupled from the leading shock (not visible) for the entirety of the tube cross-section at the axial location of detonation initiation. Between images 3 and 4, the velocity of the azimuthal detonation measured from end-view photography is 2100 m/s, while the axial velocity of the detonation measured from side-view is ~2600 m/s. A second initiation site at the 1 o'clock tube wall position is seen in image 5 end-view, although it is less evident from a side-view perspective. The two detonation fronts interact near the top of the tube. From a side view, the detonation front from the first initiation site is seen in the forefront of the image, and two bright lines are observed which correspond to the azimuthal detonation propagating along the tube back wall. The remaining azimuthally propagating detonations propagating at the tube wall are clearly seen in image 7, and a vertical bright line corresponding to the radially propagating detonation front is also observed. The end-view captures this more distinctly, showing that the detonation has nearly spanned the entire tube cross-section. Image 8 end-view shows the collision of the two detonation fronts at the 3 o'clock position, the planar detonation collision forms a horizontal bright line in the corresponding side-view image. Detonation initiation was exclusive to the channel walls for propane-oxygen at an initial pressure ≤ 5.6 kPa.

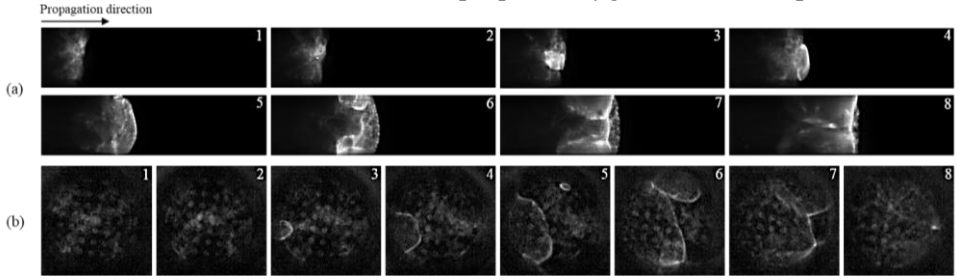

Figure 2: Simultaneous (a) side-view starting at 9.5 cm from perforated plate, field-of-view is 27.5 cm long and (b) end-view direct photography for a test with $C_3H_8 + 5O_2$ at an initial pressure of 5.5 kPa showing detonation initiation at the wall. Time between frames is 7.14 μs.

Figure 3 shows the soot foil record obtained for a $C_3H_8+5O_2$ test at an initial pressure of 5.8 kPa. The soot foil wraps around the full circumference of the tube and is 56 cm long, where the left-most edge corresponds to the perforated plate. The shock-wall collision resulting from the shocks emerging from the four groups of peripheral holes located closest to the channel wall (as discussed in *3.3.1*) is observed at the left-most edge of the foil; two red arrows indicate one of such occurrences. Such a defined imprint is not present for the shocks emerging from the periphery holes further from the channel wall due to a decreased shock strength from diffraction. Horizontal white lines (see white arrow) are generated due to the collision of shocks propagating through adjacent holes, some of which generate triple-point tracks (and associated transverse wave). The first generation of triple-point collisions corresponds to the fuzzy 'mountain peak' lines imprinted on the foil (e.g. white dotted lines). However, most of the associated triple-point tracks do not persist further downstream and as a result much of the lofted soot is scrubbed

out by the flame. A few transverse waves survive beyond the first generation of triple-point collisions and the associated triple-point tracks can be traced until these waves collide (e.g. red dotted line on the figure). Detonation is initiated by collisions between such transverse waves at two locations (D1, D2). D1 corresponds to a DDT run-up distance of 32.6 cm. A band of extremely fine cells appear next to the major triple-point tracks associated with D1, typical of a transverse detonation (see Fig. 3c-d). D2 produces an overdriven detonation but no fine cells are observed along the bounding triple point tracks (see Fig. 3b). The upper and lower triple-point track of D1 and D2 respectively collide producing fine cells characteristic of an overdriven detonation which stabilizes further downstream (λ_{CJ}= 7.6 cm [8]).

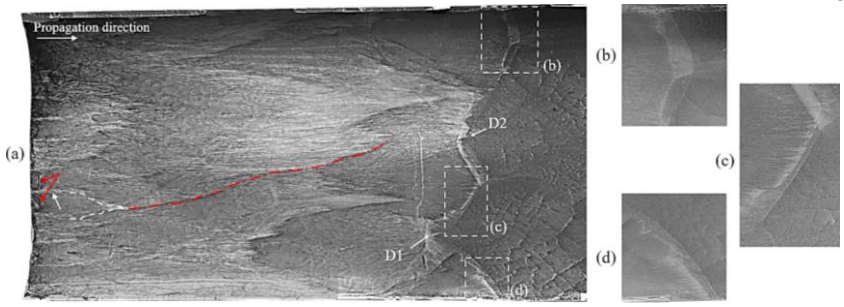

Figure 3: (a) Soot foil record for a $C_3H_8+5O_2$ test at an initial pressure of 4.8 kPa and (b-d) detailed views (corresponding to the white dotted boxes in (a)) of the detonation cell structure.

Figure 4a shows a soot foil record for a $C_3H_8+5O_2$ test performed at an initial pressure of 5.7 kPa. The foil only wrapped half the tube circumference and was oriented allowing simultaneous direct photography. The foil presented in Fig. 4a has been partially "unwrapped" to provide a clearer view of the cell structure evolution. The foil is 56 cm long and the left-most edge corresponds to the perforated plate. The foil is comparable to that in Fig. 3, and the DDT run-up distance is 20 cm.

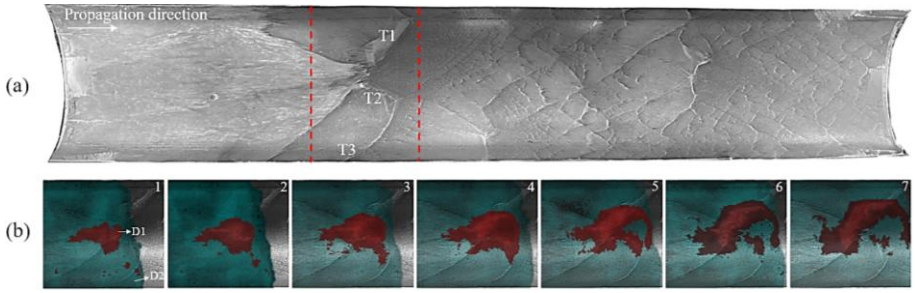

Figure 4: (a) One-half circumference soot foil record for a $C_3H_8+5O_2$ test at an initial pressure of 5.7 kPa and (b) foil as it appears in the tube, with superimposed gas chemiluminescence (blue) and soot incandescence (red) video frames. 2 μs between frames.

As the shock passes over the soot foil, soot particles are lifted and heated to high temperature by the gas products, producing an incandescence that dominates the gas chemiluminescence. Figure 4b shows the "wrapped" version of the foil, where the upstream and downstream edges correspond to the red dotted lines in Fig. 4a. Light emission from the soot foil, captured through a 430 nm narrowband filter, has been superimposed overtop foil segment between the red dotted lines in Fig. 4a. To distinguish between gas chemiluminescence and soot incandescence, two images with different intensity thresholds were artificially colored and overlaid. Lower intensity regions are colored blue and correspond to gas chemiluminescence, while higher intensity regions corresponding to soot incandescence are colored red. Significant incandescence is observed at roughly mid-height of image 1. Initiation results from the collision of transverse waves, producing an axially propagating overdriven detonation (D1). A "band" of extremely fine cells beside the major triple-point tracks (T1, T2) after the collision indicates a transverse detonation with corresponding intense light in Fig. 4b. Gas chemiluminescence is observed downstream of the detonation initiation site which provides insights regarding the shape of the turbulent flame front at the time of initiation. A third strong triple-point track (T3) associated with a second detonation front (D2) is also observed in image 1. D2 is less evident in the red superimposed image because D2 is rapidly decaying in strength, evident by the quick disappearance of the interior cell

structure. The incandescence generated in images 2 – 5 shows the detonation front bound by T1 and T2 as it propagates downstream. The velocity of the detonation front between images 3-4 and 4-5 measured at mid-height is 2800 m/s and 2600 m/s which supports that the detonation is initially overdriven (V_{CJ} = 2230 m/s). Due to a collision between T2 and T3 between images 5 and 6, a faint white line is imprinted on the foil and the detonation is overdriven to a velocity of 2400 m/s. Also, between images 5 and 6, D1 overtakes the centerline combustion front (leading edge of blue region) away from the wall. Images 6 and 7 show a bright horizontal incandescence associated with the transverse detonation propagates along the upper detonation triple-point track T1 at a velocity of 2214 m/s.

3.1.3. Tube Center Detonation Initiation

Figure 5 shows select frames from simultaneously recorded side and end-view videos for a $C_3H_8{+}5O_2$ test at an initial pressure of 6 kPa. The side-view for images 1 and 2 shows the turbulent flame structure and the distinct 'X' shock pattern is present but barely visible in image 1. In image 2 the light emission becomes more intense near the center of the channel, much like that observed in image 2 of Fig. 2 indicating shock focusing. Detonation is initiated between images 2 and 3 at the center of the tube. Recall, similar shock focusing was not sufficient to initiate detonation for the test shown in Fig. 2 for a less reactive condition. Image 3 end-view photography shows that initiation occurs at roughly the center of the tube, and the DDT distance from the perforated plate measured from side-view photography was 10.8 cm. The wave velocity obtained from the end-view images 3 and 4 is 2353 m/s towards the left side corresponds to a detonation (V_{CJ}=2232 m/s). The remainder of the wave front propagates at ~ 1600 m/s well below V_{CJ}, the reflection of which occurs at the wall on the right side between images 5 and 6. The reflection of this wave most likely started a uniform detonation front on the right wall that is observed as a planar detonation in the side view images 7 and 8 propagating at 2428 m/s.

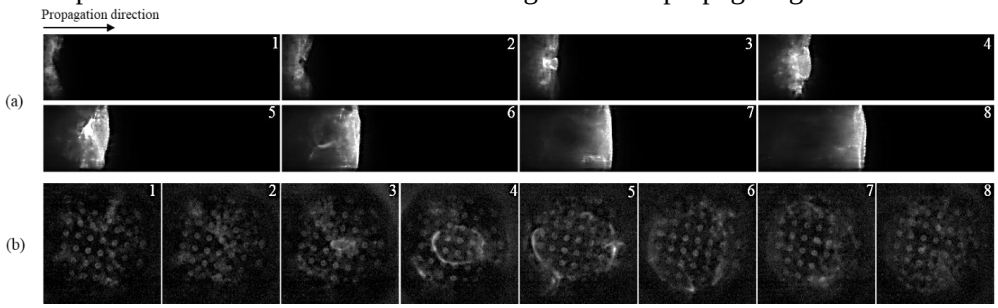

Figure 5: Simultaneous (a) side-view starting at 9 cm from perforated plate with field-of-view of 27.5 cm and (b) end-view direct photography for $C_3H_8 + 5O_2$ at an initial pressure of 6 kPa. Time between frames 7.14 μs.

3.2 Detonation Initiation Criteria

Figure 6 compares the results of detonation re-initiation after the perforated plate from the present study carried out in a round tube with the previous study done in a square channel [5] with the same 7.6 cm lateral dimension. The primary and secondary x-axes provide the number of detonation cells across the channel width (D/λ) and across the perforated plate hole diameter (d/λ), where the detonation cell sizes were obtained from Caltech detonation database [8]. The data for each mixture sets is distributed on the y-axis based on the χ parameter which is reflective of the mixture detonation stability. The square and circle symbols correspond to data acquired from the square channel and round tube respectively. The minimum pressure for prompt, delayed and no detonation re-initiation are provided for convenience. The diamond symbols represent the lowest initial pressure for which a detonation wave was produced upstream of the perforated plate. Due to a modification to the ignition system for the current study, the minimum initial pressure for $C_3H_8 + 5O_2$ was decreased to 4 kPa, compared to 6.5 kPa [5]. For propane-oxygen with and without argon-dilution the transition from delayed to prompt initiation occurred at the same critical condition d/λ=1.67 for both channel cross-sections. This emphasizes that prompt initiation is driven by transverse wave collisions generated by the decoupled detonation immediately after the perforated plate and the channel corners do not play a role. The critical d/λ in the round tube for

$2H_2+O_2+2Ar$ was slightly larger compared to the square channel. Given the limited results for this mixture, the same conclusion may be supported even though a more extensive dataset would be needed for statistical confirmation. In general, an increase in χ results in a decrease in the minimum d/λ for prompt initiation and minimum D/λ for delayed initiation.

In the square-channel experiments [5], delayed detonation initiation was observed for all mixtures at the channel boundary; for $C_3H_8+5O_2$ delayed initiation occurred both at the walls and in the corners. In the round tube, delayed initiation for $C_3H_8+5O_2$ was limited to the walls at the lowest pressures, but could occur due to symmetric shock focusing at the tube center (which was not observed in the square channel [5]) for pressures ranging from 6 kPa to 10 kPa. Delayed initiation for $C_3H_8+5O_2+4Ar$ at initial pressures less than 28 kPa was restricted to the channel corners; whereas, in the round tube for $C_3H_8+5O_2+4Ar$ detonation initiation was only observed at initial pressures greater than or equal to 28 kPa which indicates that the square channel corners are critical in promoting delayed detonation initiation for this regular cell structure mixture. A similar conclusion can be drawn for the results obtained from the limited $2H_2+O_2+2Ar$ tests performed in both channel configurations. Both argon-diluted mixtures exhibit greater detonation stability (lower χ) stoichiometric propane-oxygen. Perhaps the high temperature and pressure conditions generated in the corners are critical for initiation at lower pressures for mixtures with lower reaction temperature sensitivity (lower χ).

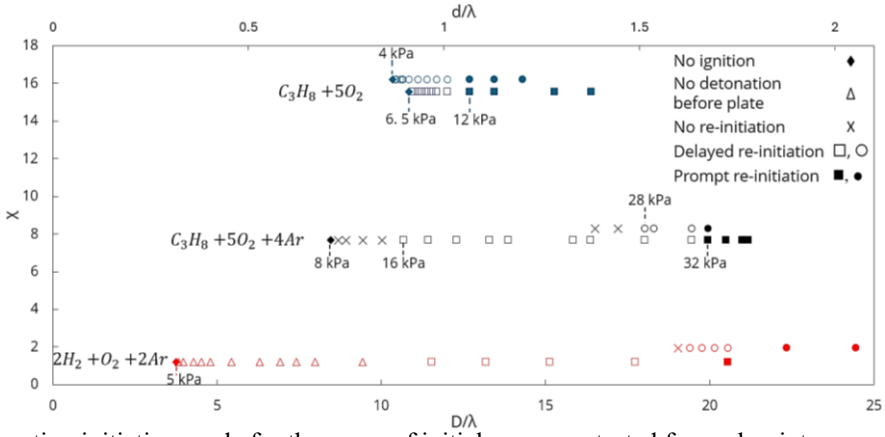

Figure 6: Detonation initiation mode for the range of initial pressures tested for each mixture grouped based on the calculated χ using SD Toolbox [9]. Round tube data from this study and square channel data from [5] denoted by round and square symbols. Note d = 6.4 mm and D = 76.2 mm.

4 Conclusions

We studied the transition to detonation downstream from a perforated plate in a 7.62 cm diameter tube, results were compared to experiments performed in a 7.62 cm cross-section square channel [5]. The critical d/λ for the transition from delayed to prompt initiation was the same for both channels indicating that prompt initiation is independent of the channel cross-section shape. Soot foil tests showed that at the lowest pressures only a few transverse waves persist far downstream from the perforated plate, and detonation initiation occurred from a singular transverse wave collision at the channel wall. From end-view chemiluminescence, the orientation of the holes of the perforated plate on shock dynamics after the perforated plate was explored. Regardless of hole orientation, shock focusing at the center of the tube followed by shock reflection at the channel wall was observed to occur periodically, in a pulsing pattern. For mixtures of sufficient reactivity, the shock collision at the center of the tube could be sufficient for detonation initiation. At lower initial pressures, initiation would often occur subsequently upon shock reflection at the tube walls. In the round tube, the critical D/λ for delayed initiation of argon-diluted mixtures matched that of the square channel once initiation was no longer exclusive to the channel corners. This result suggests that shock focusing in the channel corner is critical for regular cell structure mixtures.

References

[1] J. Chao, T. Otsuka, J.H. Lee, An experimental investigation of the onset of detonation, Proc. Combust. Inst. 30 (2005) 1889–1897.
[2] M. Saif, W. Wang, A. Pekalski, M. Levin, M.I. Radulescu, CJ deflagrations and their transition to detonation, Proc. of the Comb. Inst. 36:2771-2779, 2017.
[3] J.S. Grondin, J.H. Lee, Experimental observation of the onset of detonation downstream of a perforated plate, Shock Waves 20:381–386, 2010.
[4] V. Monnier, V. Rodriguez, P. Vidal, and R. Zitoun, Three-dimensional dynamics of detonation diffraction: effects of the tube cross-section shape, ICDERS, 2023.
[5] M. Moran, G. Ciccarelli, The transition from CJ-deflagration to detonation in a square channel, Work in Progress Poster, Int. Combustion Symp., Milan, 2024.
[6] Y. Ballossier, F. Virot, J. Melguizo-Gavilanes, Strange wave formation and detonation onset in narrow channels, J. Loss Prev. Proc. Ind. 72 (2021) 104535.
[7] J. Chambers, H. Chin, A. Poludnenko, V. Gamezo, K. Ahmed, Spontaneous runaway of fast turbulent flames for turbulence-induced DDT, Phys. Fluids 34, 015114, 2022.
[8] "Detonation Database -- Cell Size." Accessed: Nov. 26, 2024. https://shepherd.caltech.edu/detn_db/html/db_12.html
[9] J.E. Shepherd, SDToolbox, California Institute of Technology